Published for SISSA by Springer

Received: March 27, 2018
Revised: June 26, 2018
Accepted: June 27, 2018
Published: July 11, 2018

JHEP07(2018)081

Dark decay of the neutron

James M. Cline and Jonathan M. Cornell

McGill University, Department of Physics,
3600 University St., Montréal, QC H3A2T8, Canada

E-mail: jcline@physics.mcgill.ca, cornellj@physics.mcgill.ca

Abstract: New decay channels for the neutron into dark matter plus other particles have been suggested for explaining a long-standing discrepancy between the neutron lifetime measured from trapped neutrons versus those decaying in flight. Many such scenarios are already ruled out by their effects on neutron stars, and the decay into dark matter plus photon has been experimentally excluded. Here we explore the decay into a dark Dirac fermion χ and a dark photon A', which can be consistent with all constraints if χ is a subdominant component of the dark matter. Neutron star constraints are evaded if the dark photon mass to coupling ratio is $m_{A'}/g' \lesssim (45-60)\,\mathrm{MeV}$, depending upon the nuclear equation of state. g' and the kinetic mixing between U(1)$'$ and electromagnetism are tightly constrained by direct and indirect dark matter detection, supernova constraints, and cosmological limits.

Keywords: Beyond Standard Model, Cosmology of Theories beyond the SM

ArXiv ePrint: 1803.04961

Open Access, © The Authors.
Article funded by SCOAP^3.

https://doi.org/10.1007/JHEP07(2018)081

Contents

1 Introduction 1

2 Model-independent analysis 2

3 Neutron star constraints 4

4 UV model 5

5 Cosmology 7

6 Direct detection 9

7 Indirect detection 10

7.1 Constraints on g' 10

8 Kinetic mixing constraints 11

9 Conclusions 12

1 Introduction

Recently a long-standing experimental discrepancy in the lifetime of the neutron has been highlighted: the decay rate of neutrons stored in a bottle [1–5] seems to be larger than that determined by detecting the decay products from neutrons in flight [6, 7]. The difference in the associated lifetimes is $\sim 8\,\mathrm{s}$ with a 4σ tension. Ref. [8] pointed out that this could be explained by a hitherto undetected extra decay channel into dark particles, if the neutron mixes with fermionic dark matter (DM) χ whose mass is in a narrow range $m_p - m_e < m_\chi < m_n$ consistent with proton stability. The simplest decay channel, $n \to \chi\gamma$, comes from the transition magnetic moment interaction $\bar{n}\sigma_{\mu\nu}\chi F^{\mu\nu}$ induced by the n-χ mixing. This has already been ruled out by a null search for the monochromatic photon [9]. (It was also argued that any such solution of the lifetime problem would exacerbate tensions in discrepant determinations of the neutron axial-vector coupling g_A [10]).

Even if the new decay channel is completely invisible, for example $n \to \chi\phi$ where ϕ is a dark scalar, neutron stars ostensibly rule out the scenario [11–13], since χ typically has a much softer equation of state than nuclear matter at high density. The conversion of n to χ in a neutron star (NS) then leads to the maximum possible mass of the star being well below the largest values observed (near $2M_\odot$). Ref. [11] pointed out that this constraint can be evaded if χ has additional pressure from the repulsive self-interactions that would come from dark photon (A') exchange, if the mass-to-coupling ratio $m_{A'}/g'$ is sufficiently large, though the minimum required value was not determined. One of our goals is to find this value.

JHEP07(2018)081

This suggests that a consistent picture can be made if the new dark decay channel is $n \to \chi A'$. Astrophysical and cosmological considerations substantially constrain DM in the mass range required to explain the neutron lifetime anomaly. However, χ could still be a subdominant component of the total dark matter.

In the following, we start by deriving constraints on our scenario that depend only upon the low-energy particle content at the GeV scale or below, in section 2. This is followed by analysis of the effects upon neutron stars, section 3, where an upper bound on $m_{A'}/g'$ is derived. We introduce the microscopic renormalizable model in section 4 and discuss the implications for cosmology in section 5. The constraints from direct and indirect detection are derived in sections 6 and 7. Various constraints on the kinetic mixing parameter between the U(1)′ and electromagnetic U(1) field strengths are compiled in section 8, followed by our conclusions, section 9.

2 Model-independent analysis

Before presenting a more complete particle physics model, we start with the low-energy effective Lagrangian that contains almost everything needed for the phenomenology. It has mixing of the Dirac χ with the right-handed component of the neutron (this restriction does come from UV considerations, to be explained later) and the usual terms for χ interacting with a dark photon A':

$$\begin{aligned}\mathcal{L}_{\text{eff}} = {} & \bar{\chi}(i\not{D} - m_\chi)\chi + \bar{n}\left(i\not{\partial} - m_n + \mu_n \sigma^{\mu\nu} F_{\mu\nu}\right) n - \frac{1}{4} F'_{\mu\nu} F'^{\mu\nu} \\ & - \frac{1}{2} m_{A'}^2 A'^\mu A'_\mu - \delta m\, \bar{n}_R \chi_L + \text{h.c.} - \frac{\epsilon}{2} F_{\mu\nu} F'^{\mu\nu} \end{aligned} \tag{2.1}$$

where $D_\mu = \partial_\mu - i g' A'_\mu$ and μ_n is the neutron magnetic dipole moment. Kinetic mixing with the photon is included so that A' will eventually decay to photons through a loop diagram, or electrons if $m_{A'} > 2m_e$. We assume that χ is a Dirac particle, since UV models in which χ is Majorana generically lead to dinucleon decays such as ${}^{16}\text{O}(pp) \to {}^{14}\text{C}\pi^+\pi^-$ [14].

Diagonalization of the n-χ mass matrix requires rotations of (n_R, χ_R) and (n_L, χ_L) respectively by angles θ_R and θ_L with

$$\theta_R \cong \frac{m_n \delta m}{m_n^2 - m_\chi^2}, \quad \theta_L \cong \frac{m_\chi \delta m}{m_n^2 - m_\chi^2} \tag{2.2}$$

Since m_χ is close to m_n, these angles are roughly equal, $\theta = \theta_R \cong \theta_L \cong \delta m/(2(m_n - m_\chi))$. Going to the mass basis, the $\bar{\chi}\not{A}'\chi$ interaction then leads to an off-diagonal term,

$$-\, g' \theta\, \bar{n} \not{A}' \chi + \text{h.c.} \tag{2.3}$$

that leads to the dark decay $n \to \chi A'$ assuming that $m_n > m_\chi + m_{A'}$. Since A' is unstable because of kinetic mixing with the photon, we assume that it is either sufficiently long-lived to escape detection, or its decay products e^+e^- or 3γ have not yet been excluded by observations of neutron decay.

JHEP07(2018)081

The decay rate for $n \to \chi A'$ can be expressed in terms of the ratios $x = (m_n - m_\chi)/m_n$ and $r = m_{A'}/(m_\chi - m_n)$, where $x \in [0,\, 1.78 \times 10^{-3}]$ (the upper limit is imposed by the stability of ^{9}Be [8, 15]) and $r \in [0, 1]$:

$$\Gamma(n \to \chi A') \cong \frac{g'^2\theta^2 m_n x}{2\pi r^2}\,(1-r^2)^{3/2} \cong \frac{g'^2(\delta m)^2 m_n}{8\pi m_{A'}^2}\,x\,(1-r^2)^{3/2} \tag{2.4}$$

where we have ignored negligible higher order corrections in x, and in the second line eliminated θ using (2.2). The limit $m_{A'} \to 0$ is not singular, despite appearances, when A' gets its mass from spontaneous symmetry breaking, as we explicitly show in section 4. $g'\delta m/m_{A'}$ remains finite in this limit.

To resolve the neutron lifetime discrepancy, the partial width must be 7×10^{-30} GeV [8]. For definiteness, we adopt the reference value $m_\chi = 937.9\,\text{MeV}$, which maximizes the dark decay rate with $m_n - m_\chi \cong 1.67\,\text{MeV}$. Moreover we consider two benchmark values of $m_{A'} = 1.35\,\text{MeV}$ and $0.5\,\text{MeV}$ to illustrate the differences between being above or below the $2m_e$ threshold for A' decays. We refer to the two cases as scenarios **A** and **B**, respectively. We then find

$$\frac{g'\delta m}{m_{A'}} \cong 7.2\,(3.5) \times 10^{-13}, \quad \text{scenario } \mathbf{A}\ (\mathbf{B}) \tag{2.5}$$

With the neutron star bound $m_{A'}/g' \lesssim 60\,\text{MeV}$ to be derived in section 3, this implies $\delta m < 4\,(2) \times 10^{-11}\,\text{MeV}$, which gives a limit on the mixing angle

$$\theta < 1.3 \times 10^{-11}\,(6.3 \times 10^{-12}) \tag{2.6}$$

for the two scenarios. Although the decay $\chi \to p e^- \bar{\nu}_e$ is kinematically allowed if $m_\chi > m_p + m_{e^-} = 938.8\,\text{MeV}$, such a small mixing endows χ with a lifetime well beyond the age of the universe. Therefore χ is always a component of the DM, even when it is not absolutely stable.

To satisfy the constraint on $n \to \chi\gamma$ from ref. [9], δm must be smaller by a factor of approximately 2.6 than the value needed for explaining the lifetime discrepancy in terms of this decay.[1] Using the value of δm determined in [8], this leads to the limit

$$\delta m \lesssim 3.6 \times 10^{-11}\,\text{MeV} \tag{2.7}$$

which is similar to those coming from (2.5) combined with the bound on $m_{A'}/g'$ from neutron stars, that we discuss in the next section. This result can also be translated into to a limit on g' using eq. (2.5):

$$g' \gtrsim 27\,(4.9) \times 10^{-3}, \quad \text{scenario } \mathbf{A}\ (\mathbf{B}) \tag{2.8}$$

[1] Ref. [9] does not quite exclude the model with minimum $m_\chi = 937.9$ that we consider, which would lead to a photon of energy 1.66 MeV. The maximum photon energy excluded in [9] is 1.62 MeV. We assume that this narrow window will be closed by a wider search.

JHEP07(2018)081

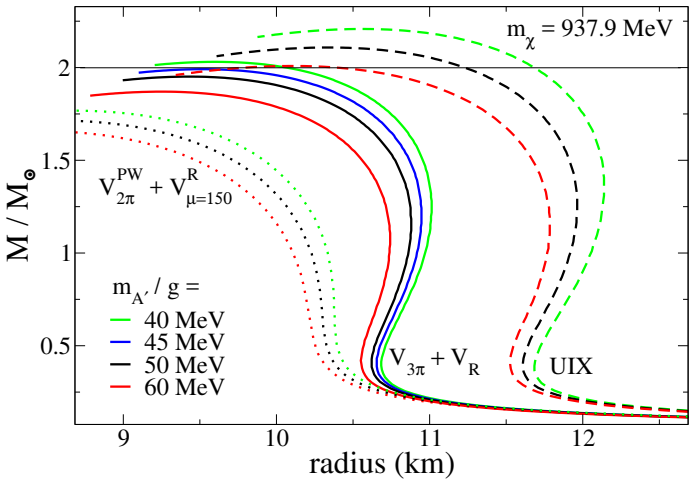

Figure 1. Neutron star mass-radius curves showing the effect of dark matter pressure for several values of the dark photon mass to charge ratio $m_{A'}/g'$, and several nuclear equations of state; see text for details.

3 Neutron star constraints

Although the mixing angle (2.2) between the neutron and χ is very small, it is sufficient to bring the two into chemical equilibrium in neutron stars [11]. If χ is noninteracting, then dense neutron matter converts to χ in order to lower the pressure. Integrating the Tolman-Oppenheimer-Volkoff equations [16, 17] that determine the NS structure, one finds that the maximum NS mass attained as a function of its radius falls below the largest observed masses, close to $2M_\odot$ [18]. Ref. [11] notes that this can be avoided if $m_\chi > 1.2\,\mathrm{GeV}$, which would preclude the $n \to \chi$ decays, or if the DM has repulsive self-interactions, such as would arise from Coulomb repulsion if χ is charged under a U(1)$'$ gauge symmetry. If the U(1)$'$ is spontaneously broken as we assume, so the gauge boson is massive, this reduces the pressure since the range of the interaction becomes $m_{A'}^{-1}$. We would like to know how large $m_{A'}/g'$ can be while still attaining a 2 solar mass neutron star.

We have followed the procedure outlined in [11] to answer this question. The DM is treated as a degenerate Fermi gas with self-interactions, so that its energy density is given by

$$\rho_\chi = \frac{1}{\pi^2}\int_0^{k_F} dk\, k^2 \sqrt{k^2 + m_\chi^2} + \frac{g'^2}{2m_{A'}^2} n_\chi^2 \tag{3.1}$$

where k_F is the Fermi momentum and $n_\chi = k_F^3/3\pi^2$. k_F is determined by the chemical potential

$$\mu_\chi = \sqrt{k_F^2 + m_\chi^2} + \frac{g'^2}{m_{A'}^2} n_\chi \tag{3.2}$$

The DM pressure is given by $p_\chi = -\rho_\chi + \mu_\chi n_\chi$. Chemical equilibrium implies that μ_χ equals the baryon (neutron) chemical potential μ_B, which is determined by the nuclear equation of state (EoS). χ will be produced at any radius within the NS where $\mu_B > m_\chi$.

JHEP07(2018)081

The DM contributions to pressure and energy density are added to those of the nuclear matter to find the modified EoS.

The nuclear EoS can be specified in terms of the internal energy of a nucleon, $E_n(x)$, as a function of the dimensionless nuclear density $x = n_n/n_0$, where $n_0 = 0.16\,\mathrm{fm}^{-3}$ is the saturation density. We adopt a polytropic EoS of the form [19]

$$E_n(x) = ax^\alpha + bx^\beta \tag{3.3}$$

that has been fit to the results of quantum Monte Carlo calculations incorporating realistic 3-nucleon forces. The nuclear pressure is given by $p_n = n_n^2 dE_n/dn = n_0(a\alpha x^\alpha + b\beta x^\beta)$, and the energy density is $\rho_n = n_n(m_n + E_n)$. The chemical potential is then $\mu_B = (p_n + \rho_n)/n_n$. This approximation is adequate at high densities near the center of the NS, but at some radius as the density increases, the effect of nuclear binding becomes important, allowing μ_B to fall below m_n (which otherwise would not happen) and also m_χ. At this radius the χ density falls to zero and the dark matter can no longer soften the EoS. We model this effect by subtracting the binding energy $E_b = 8\,\mathrm{MeV}$ (which follows from the semi-empirical mass formula of nuclear physics [20]) from μ_B.

Carrying out the above procedure we find the NS mass as a function of its radius for a range of central densities of the NS, to produce the mass-radius curves corresponding to different values of $m_{A'}/g'$. The results are shown in figure 1 for several equations of state from ref. [19]. The solid lines (labeled $V_{3\pi} + V_R$) correspond to a moderately stiff EoS with $a\,(b) = 13.0\,(3.21)\,\mathrm{MeV}$, $\alpha\,(\beta) = 0.49\,(2.47)$, while the dashed ones (labeled UIX) pertain to a more stiff EoS with $a\,(b) = 13.4\,(5.62)\,\mathrm{MeV}$, $\alpha\,(\beta) = 0.514\,(2.436)$. The dotted curves (labeled $V_{2\pi}^{PW} + V_{\mu=150}^{R}$) are for a soft EoS that cannot produce a $2M_\odot$ NS even in the absence of dark matter. To obtain a maximum mass compatible with $2M_\odot$ requires

$$\frac{m_{A'}}{g'} \lesssim (45 - 60)\,\mathrm{MeV} \tag{3.4}$$

depending upon the nuclear EoS.

4 UV model

Direct and indirect signals of subdominant χ dark matter can depend upon details of the particle physics beyond the low-energy effective description (2.1). In particular a light scalar particle must be in the spectrum, to account for the mass of A' through the Higgs mechanism. Here we build a minimal model that could consistently give rise to the Lagrangian (2.1). It is strongly constrained by the gauge symmetries, giving us little freedom in its construction. We demand that the U(1)$'$ gauge symmetry be only spontaneously broken, requiring a scalar ϕ that carries U(1)$'$ charge, with a potential

$$V = \lambda\left(|\phi|^2 - v'^2\right)^2 \ . \tag{4.1}$$

Moreover a renormalizable interaction of χ with a quark needs a scalar Φ_1 that is fundamental under SU(3)$_c$ and also charged under U(1)$'$. To connect this to the other quarks in

JHEP07(2018)081

the neutron, a second triplet scalar Φ_2, neutral under U(1)$'$ is needed, along with a cubic scalar interaction,

$$\mu\, \Phi_{1,a}\, \Phi_2^{*a}\, \phi \tag{4.2}$$

where μ has dimensions of mass. To satisfy SU(2)$_L$ gauge symmetry we take the triplets to couple only to right-handed quarks,

$$\lambda_1\, \bar{d}^a P_L \chi\, \Phi_{1,a} + \lambda_2\, \epsilon^{abc}\, \bar{u}_a^c P_R\, d_b\, \Phi_{2,c}\,. \tag{4.3}$$

Φ_1^*, χ and ϕ all carry unit dark U(1)$'$ charge with coupling g'. The vacuum expectation value (VEV) of ϕ breaks U(1)$'$ and gives the dark photon mass $m_{A'} = g'v'$.

We can consistently assign baryon number to all the new fields: $B_\chi = 1$, $B_{\Phi_1} = B_{\Phi_2} = -2/3$, $B_\phi = 0$. Therefore the model is free from constraints on B-violating processes such as neutron-antineutron oscillations and dinucleon decay. The need to kinematically forbid decays of ^{9}Be (if $m_\chi \geq 937.9\,\mathrm{MeV}$) also stabilizes the proton and forbids possibly problematic decays of Λ baryons to final states including a χ, such as $\Lambda_0 \to \chi \bar{K}_0$, as well as decays of light mesons to $\bar{\chi}\chi$.

The virtual exchange of the heavy Φ_2 generates a contact interaction that can be Fierz-transformed to

$$\mathcal{L}_c = \frac{|\lambda_2|^2}{2m_{\Phi_2}^2}(\bar{u}_R\gamma_\mu u_R)(\bar{d}_R\gamma^\mu d_R) \tag{4.4}$$

The coefficient is constrained by measurements of dijet angular distributions at the LHC [21], $m_{\Phi_2}/\lambda_2 \gtrsim 4\,\mathrm{TeV}$.

The scalar triplets, which could decay to two jets or a jet and missing energy, must be at the TeV scale to satisfy LHC constraints on their direct production. [22]. Integrating them out generates the effective interaction

$$\eta\, \bar{n}\phi^* P_L \chi \tag{4.5}$$

with

$$\eta = \frac{\beta\mu\lambda_1\lambda_2}{m_{\Phi_1}^2 m_{\Phi_2}^2} \cong 2.4\times 10^{-12}\left(\frac{\lambda_1\lambda_2\,\mu}{\mathrm{TeV}}\right) \tag{4.6}$$

where $\beta \cong 0.014\,\mathrm{GeV}^3$ from lattice QCD [23], and the scalar masses saturate the ATLAS limit $m_{\Phi_i} > 1.55\,\mathrm{TeV}$. When ϕ gets its VEV, the off-diagonal mass $\delta m = \eta v'$ between n_R and χ_L is generated. Since $m_{A'}/g' = v'$, we can combine (4.6) with (2.5) to determine

$$\lambda_1\lambda_2\,\mu \cong (140 - 290)\,\mathrm{GeV} \tag{4.7}$$

If $\lambda_1 \sim \lambda_2 \sim 0.4$ (consistent with the previous LHC limits), then μ can be near the TeV scale, like the triplet scalar masses. But v' must be at the much lower scale $\lesssim 60\,\mathrm{MeV}$ from (3.4).

The scalar ϕ cannot be arbitrarily heavy. Its mass is $m_\phi = 2\sqrt{\lambda}v$ hence $m_\phi/m_{A'} = 2\sqrt{\lambda}/g'$. The upper limit from partial wave unitarity is $\lambda \leq 4\pi$. For our benchmark models this would give a mass of order $m_\phi \sim 70\,\mathrm{MeV}$. The decay channel $n \to \chi\phi$ is closed, and only leads to a subdominant mode $n \to \chi A' A'$ through virtual ϕ exchange. However, when

JHEP07(2018)081

$m_\phi \gg m_{A'}$, the scalar decays via $\phi \to A'A'$, and as $\chi\bar{\chi} \to \phi A'$ is an allowed process, it can have non-negligible effects on both cosmology and indirect detection signals. For simplicity we assume that λ is large and m_ϕ takes the benchmark value of 70 MeV. This is large enough so that we can ignore the effects of ϕ on neutron decay, but we will consider its effect on DM physics. We also note the cubic coupling (4.2) could lead to interesting cascade decays of the heavier of the two color triplet scalars Φ_i produced at the LHC, but this is beyond the scope of the present work.

5 Cosmology

In the limit of low relative velocity, the cross section for $\chi\chi$ elastic scattering by dark photon exchange takes the form

$$\sigma_{\chi\chi} = \frac{g'^4 m_\chi^2}{4\pi m_{A'}^4} \gtrsim 2 \times 10^{-24}\,\mathrm{cm}^2\,, \tag{5.1}$$

with the lower bound derived using the limit on $m_{A'}/g'$ from neutron stars in eq. (3.4). It is interesting that the lowest allowed value of $\sigma_{\chi\chi}$ is of the appropriate strength to explain observations of astrophysical structure on small scales that are in tension with the predictions of cold dark matter [24]. However constraints from the Cosmic Microwave Background (CMB) and astrophysics discussed in section 7 will ultimately limit χ to be a small fraction of the total DM, preventing our model from addressing these issues.[2] Larger values of $\sigma_{\chi\chi}$ could run afoul of constraints on DM self-scattering from the Bullet Cluster [26], but this limit is avoided when χ is subdominant; up to around 10% of the total DM population might have such strong self-interactions [27, 28].

The relic density of χ is determined by $\chi\bar{\chi} \to A'A'$ and $\chi\bar{\chi} \to \phi A'$ annihilations, assuming there is no asymmetry between χ and $\bar{\chi}$. There are also a tree level process that give annihilation into quarks, $\chi\bar{\chi} \to d\bar{d}$, but this process is greatly suppressed by the TeV scale mass of the Φ_2. The cross sections for the relevant processes are given by [29]

$$\langle \sigma_{\mathrm{ann}} v_{\mathrm{rel}} \rangle_{\chi\bar{\chi}\to A'A'} = \frac{g'^4}{16\pi m_\chi^2} \frac{(1-\eta_{A'})^{3/2}}{(1-\eta_{A'}/2)^2} \tag{5.2}$$

$$\langle \sigma_{\mathrm{ann}} v_{\mathrm{rel}} \rangle_{\chi\bar{\chi}\to\phi A'} = \frac{g'^4}{4096\pi m_\chi^2} \frac{\sqrt{(\eta_\phi - \eta_{A'} - 4)^2 - 16\eta_{A'}}\left((\eta_\phi - \eta_{A'} - 4)^2 + 32\eta_{A'}^2\right)}{(1-\eta_{A'}/4)^2}\,, \tag{5.3}$$

where $\eta_{A',\phi} = m_{A',\phi}^2/m_\chi^2$. For χ to make up all of the DM, the total annihilation cross section should be close to $10^{-25}\mathrm{cm}^3/\mathrm{s}$ [30]. If $m_{A'} \ll m_\chi$, $m_\phi = 70\,\mathrm{MeV}$, and χ constitutes less than 10% of the total DM, we need a 10 times larger cross section, leading to a lower bound of $g' > 0.041$. If this bound were saturated, then the NS limit (3.4) would read $m_{A'} < 2.5\,\mathrm{MeV}$. For a strong coupling $g' = 1$, the χ relic density would be 3×10^{-7} of the total DM density.

[2] For a more complicated dark sector model which could explain both the neutron lifetime puzzle and small scale structure issues, see [25].

JHEP07(2018)081

Since χ is a Dirac particle, it is possible that it has an asymmetry from some unknown mechanism operating in the early universe. Then it would be possible to have large g' and a more significant fraction of χ being the dark matter. Moreover, if the asymmetric component number density happens to be close to the symmetric contribution,[3] then one CP state of χ (either χ or its antiparticle) will have a suppressed density, which could weaken indirect detection constraints. We do not pursue this loophole in the present work, but it should be kept in mind.

χ and A' chemically decouple at a dark sector temperature of $m_\chi/30 \approx 31\,\mathrm{MeV}$. At this time the A' are still relativistic with a large number density, which can lead to several problems: if they decay during the time of Big Bang Nucleosynthesis (BBN) their energetic decay products can disturb the production of light nuclei by diluting the baryon-photon ratio as well as causing photodissociation of the nuclei, and decays during and after recombination can distort the CMB temperature fluctuations. Moreover when the dark photons become non-relativistic, an early period of matter-domination can occur which would change the expansion rate of the universe and cause further problems for BBN.

To avoid these issues, we follow [31] and require the dark photons to decay before they exceed half the energy density of the universe. The temperature of the SM photon bath at the time this occurs was shown to be

$$T_{\mathrm{dom}} \approx \frac{4 m_{A'} Y_{A'}}{3 f} \tag{5.4}$$

where $Y_{A'} = n_{A'}/s_{SM}$ at χ freeze-out and $f = 1/2$ is the fraction of the universe's energy density made up of dark photons. $Y_{A'}$ is given by

$$Y_{A'} = \frac{45\zeta(3)}{2\pi^4} \frac{\tilde{g}_D}{\tilde{g}_{SM}}\,, \tag{5.5}$$

where $\tilde{g}_D/\tilde{g}_{SM}$ is the ratio of relativistic degrees of freedom in the dark sector to that of the SM sector when the two sectors thermally decouple. As the regions of parameter space we are interested in lead to small scattering cross sections between dark and SM particles, we assume that the two sectors thermally decouple when all species are relativistic, so $\tilde{g}_D = 8$, $\tilde{g}_{SM} = 106.75$, and $Y_{A'} \approx 0.02$. We then require the lifetime $\tau_{A'}$ to be less than $H^{-1}(T_{\mathrm{dom}})$, the inverse Hubble rate at this temperature. This leads to constraints on the kinetic mixing parameter ϵ that we present in section 8. We emphasize that the method we have used here to estimate the cosmological constraints on the dark photon lifetime is rough, and more detailed studies similar to those undertaken in [32–35] are needed to determine this limit with greater precision.

Finally, DM annihilation close to recombination can also lead to distortions of the CMB anisotropies. Based on searches for this effect in temperature and polarization data, the *Planck* collaboration has determined the following 95% CL constraint [36]:

$$f_{\mathrm{eff}} \left(\frac{\Omega_\chi}{\Omega_{DM}}\right)^2 \frac{\langle \sigma_{\mathrm{ann}} v_{\mathrm{rel}} \rangle}{m_\chi} < 8.2 \times 10^{-28}\ \mathrm{cm}^3/\mathrm{s/GeV} \tag{5.6}$$

[3] If $n_\chi > n_{\bar{\chi}}$, we define $n_\chi = n_S + n_A$ and $n_{\bar{\chi}} = n_S - n_A$, where n_S and n_A are the number densities of the symmetric and anti-symmetric components respectively.

JHEP07(2018)081

where $f_{\rm eff}$ is an efficiency parameter that depends on the spectrum of injected electrons and photons, while Ω_{DM} and Ω_χ denote the ratio of the energy densities of the total dark matter and χ, respectively, to the critical density. For $m_\chi = 937.9\,\mathrm{MeV}$, $f_{\rm eff}$ is approximately 0.5 for DM annihilations to $2e^+e-$ or $3e^+e-$ final states, and 0.4 for annihilation to 6γ or 9γ final states [37]. Therefore $(\Omega_\chi/\Omega_{DM})^2\langle\sigma_{\rm ann}v_{\rm rel}\rangle \lesssim 1.5\times10^{-27}\ \mathrm{cm}^3/\mathrm{s}$ for scenario **A** (A' decays to e^+e^-), while $(\Omega_\chi/\Omega_{DM})^2\langle\sigma_{\rm ann}v_{\rm rel}\rangle \lesssim 1.9\times10^{-27}\ \mathrm{cm}^3/\mathrm{s}$ for scenario **B** (A' decays to 3γ).

6 Direct detection

Because of kinetic mixing, A' couples to standard model (SM) particles of charge e with strength ϵe. The cross section for χ to scatter on protons is

$$\sigma_{\chi p} = \frac{4\alpha(g'\epsilon)^2\,\mu_{p\chi}}{m_{A'}^4} \tag{6.1}$$

where $\mu_{p\chi} = 469\,\mathrm{MeV}$ is the reduced mass of χ and the proton. The CRESST-III experiment [38] sets a limit of $10^{-38}\,\mathrm{cm}^2$ for scattering on nucleons at $m_\chi \cong 1\,\mathrm{GeV}$, which is relaxed by a factor of ~ 2 for our model where only protons scatter. This leads to the constraint

$$g'\epsilon < 9.85\times10^{-11}\left(\frac{m_{A'}}{\mathrm{MeV}}\right)^2\left(\frac{\Omega_{DM}}{\Omega_\chi}\right)^{1/2}. \tag{6.2}$$

A similar, but weaker bound, arises from χ-electron scattering, which has been constrained using XENON100 data in ref. [39].

Mixing of χ with the neutron leads to scattering mediated by the strong interactions of the neutron with nucleons, of order $\theta^4\,\sigma_{np}$, where $\sigma_{np} \cong 20\,\mathrm{b}$ is the low-energy cross section for neutron-proton scattering. In view of (2.6), $\theta^4\,\sigma_{np} < 10^{-67}\,\mathrm{cm}^2$, far from observability. In models with $m_\chi > m_n$, as suggested in ref. [11] for evading the NS constraint, an inelastic $\chi N \to nN$ cross section of order $\theta^2\,\sigma_{np} \sim 10^{-45}\,\mathrm{cm}^2$ would arise, with a highly distinctive signature of large energy deposited in the target material. This is still 7 orders of magnitude below current sensitivity of ordinary elastic scattering, but the large release of energy might make it more observable.

In addition to these contributions that only depend upon the low-energy effective description (2.1), exchange of the heavy colored scalar Φ_1 in the UV model leads to scattering of χ on down quarks, which after Fierz-transforming comes from the operator

$$\frac{\lambda_1^2}{2m_{\Phi_1}^2}(\bar\chi_L\gamma^\mu\chi_L)(\bar d_R\gamma_\mu d_R) \tag{6.3}$$

The vector part of the quark current is simply related to that of nucleons (counting the number of down quarks in the nucleon). The corresponding cross section is $\lesssim 10^{-40}\,\mathrm{cm}^2$, several orders of magnitude below the current limit.

JHEP07(2018)081

7 Indirect detection

Indirect DM searches can give strong limits the on annihilation rate of χ particles. In particular scenario **B**, where $A' \to 3\gamma$, could lead to significant fluxes of gamma-rays from nearby dwarf spheroidal galaxies, and the *Fermi*-LAT collaboration has searched for this excess emission [40]. The spectrum of photons from a single decay of an A' (in the rest frame of the A') is given by [41]

$$\frac{dN}{dE'} = \frac{16E'^3}{17m_{A'}^4}\left[1715 - 6210\frac{E'}{m_{A'}} + 5838\left(\frac{E'}{m_{A'}}\right)^2\right] \tag{7.1}$$

for $0 \leq E' \leq m_{A'}/2$. The spectrum of photons from the annihilation $\chi\bar{\chi} \to A'A'$ (in the center of mass frame of the two annihilating particles) is then given by the boost equation

$$\frac{dN}{dE} = \frac{2}{(x_+ - x_-)}\int_{Ex_-}^{Ex_+}\frac{dE'}{E'}\frac{dN}{dE'}, \tag{7.2}$$

where $x_\pm = m_\chi/m_{A'} \pm \sqrt{(m_\chi/m_{A'})^2 - 1}$. In principle, annihilations of $\chi\bar{\chi}$ to $\phi A'$ will also have some effect on the shape of the average photon spectrum, but for the regions of parameter space of interest the branching fraction to the $\phi A'$ final state is less than 1/5 (see eqs. (5.2) and (5.3)). Therefore we make the approximation that dN/dE is determined solely by annihilations of $\chi\bar{\chi}$ to $A'A'$. With this spectrum we can determine the expected flux from a particular galaxy. Using the `gamLike` code [42], we calculate a likelihood function based on 6 years of *Fermi*-LAT observations of 15 dwarf spheroidal galaxies. With this likelihood we find that the quantity $(\Omega_\chi/\Omega_{DM})^2\langle\sigma_{\rm ann}v_{\rm rel}\rangle < 2.8 \times 10^{-28}$ cm^3/s at 95% CL for 6-photon final states.

Scenario **A**, in which the dark photons decay to electron positron pairs, could in theory give a large flux of positrons which could be detected by *Voyager* [43] and the AMS-02 [44, 45] experiment. However, it was shown in [46] that significant uncertainties in the model of cosmic-ray propagation make it difficult to reliably constrain dark matter candidates with masses less than a GeV via these observations, so we do not consider them further. Limits can also be placed on the $\chi\bar{\chi}$ annihilation rate in this scenario with *Fermi* observations of dwarf spheroidal galaxies, but these limits are subdominant to those from observations of the CMB, which we discussed in section 5.

7.1 Constraints on g'

As $m_{A'} \ll m_\chi$, the DM annihilation cross section is subject to large Sommerfeld enhancement at small relative velocities. This leads to an enhanced annihilation rate in dwarf spheroidal galaxies and at the time of recombination. The enhanced cross section is given by $\langle\sigma_{\rm ann}v_{\rm rel}\rangle = S\langle\sigma_{\rm ann}v_{\rm rel}\rangle_0$, where $\langle\sigma_{\rm ann}v_{\rm rel}\rangle_0$ is the sum of eqs. (5.2) and (5.3) and the Sommerfeld factor is approximately [50]

$$S = \left|\frac{\Gamma(a_-)\Gamma(a_+)}{\Gamma(1+2iu)}\right|^2 \tag{7.3}$$

JHEP07(2018)081

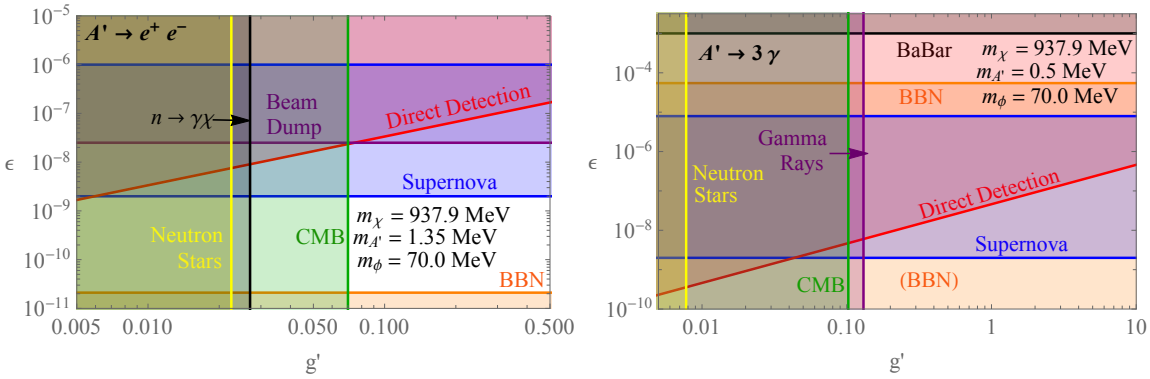

Figure 2. Limits on g' and ϵ. All shaded regions are excluded. The left plot shows the constraints on the parameter space when $m_{A'} = 1.35\,\text{MeV}$ and the dark photon decays nearly entirely to electron pairs while the right plot shows limits for when $m_{A'} = 0.5\,\text{MeV}$ and the predominant decay is to 3 photons. Constraints shown include those from direct detection with the CRESST-III experiment [38] (red; see section 6), the maximum allowed neutron star mass (yellow; see section 3), distortions of the CMB anisotropy power spectrum (green; see section 7.1) from χ annihilations [36], observations of the neutrinos from supernova 1987A [47] (blue; see section 8), BBN constraints on the decay rate of the dark photons (orange; see section 5), results from the E137 beam dump experiment [48] (purple, left plot; see section 8), *BaBar* searches for dark photon production [49] (black, right plot; see section 8), and observations of gamma rays from dwarf spheroidal galaxies with the *Fermi*-LAT [40] (purple, right plot; see section 7.1). The black shaded region in the left plot corresponds to values of g' that cannot explain the neutron lifetime discrepancy due to constraints from searches for neutron decays to a photon and invisible particle [9] (see section 2).

with $a_\pm = 1 + iu\left(1 \pm \sqrt{1 - x/u}\right)$, $x = g'^2/4\pi\beta$, $u = 6\beta m_\chi/\pi^2 m_{A'}$, and $\beta = v_{\text{rel}}/c$. For all of the dwarf spheroidal galaxies, we make the approximation $\beta \sim 10^{-4}$ (for a compilation of the velocity dispersions in each dwarf spheroidal of interest, see [51]) and we take $\beta \sim 10^{-8}$ at times around recombination.

Increasing g' ultimately reduces the expected signal in searches for DM annihilation, as the increase in the annihilation rate from the increased cross section is more than offset by the reduced χ relic density. For scenario **A** (A' decays to e^+e^-), the CMB constraints described in section 5 limit $g' \gtrsim 0.07$, so χ can be no more than 1.2% of the total DM, while for scenario **B** (A' decays to 3γ), $g' > 0.11$. For scenario **B**, the gamma-ray limits are even stronger, with g' limited to values greater than 0.14. This corresponds to χ making up only 0.08% of the total DM. These limits are displayed in figure 2. Lowering the mass of the dark photon increases the Sommerfeld enhancement and shifts the limits on g' to higher values, as more suppression of the χ relic density is needed to avoid these constraints.

8 Kinetic mixing constraints

The *BaBar* experiment has searched for production of A'-photon pairs in $e+$ $e-$ collisions, with the A' taken to decay to invisible particles [49]. This leads to the constraint $\epsilon < 10^{-3}$. Since the dark photon in our model will decay outside the detector when $\epsilon = 10^{-3}$, this limit applies here. Further direct search limits come from beam dump experiments, where dark photons with mass $\lesssim 2\,\text{MeV}$ can be produced (and detected if $m_{A'} > 2m_e$). Ref. [48] finds

JHEP07(2018)081

a limit of $\epsilon < 2.5 \times 10^{-8}$ from the E137 experiment. In addition, if A' is emitted copiously from supernovae, the observed emission of neutrinos from supernova 1987A would have been attenuated. This robustly excludes the overlapping range $\epsilon \in [2 \times 10^{-9}, 1 \times 10^{-6}]$ [47] (see also [52, 53]). If $m_{A'}$ is below the $2m_e$ threshold, the beam dump limits do not apply, and the supernova limits shift to $\epsilon \in [2 \times 10^{-9}, 8 \times 10^{-6}]$.

A lower bound on ϵ comes from the requirement that A' decays sufficiently fast (before recombination) so as not to disturb the CMB. For scenario **A**, the width of the dominant $A' \to e^+e^-$ decay and corresponding lifetime are given by

$$\begin{aligned} \Gamma_{e^+e^-} &= \frac{\alpha\epsilon^2}{3\, m_{A'}} \left(m_{A'}^2 + 2m_e^2\right) \left(1 - 4m_e^2/m_{A'}^2\right)^{1/2} \\ \tau_{e^+e^-} &\cong 24 \left(\frac{10^{-10}}{\epsilon}\right)^2 \mathrm{s}\,. \end{aligned} \tag{8.1}$$

Using the rate for $A' \to 3\gamma$ from [41], the lifetime for the A' when $m_{A'} < 2m_e$ is

$$\tau_{3\gamma} \cong 2 \times 10^{12}\,\mathrm{s} \left(\frac{10^{-10}}{\epsilon}\right)^2 \left(\frac{1\,\mathrm{MeV}}{m_{A'}}\right)^9 . \tag{8.2}$$

The exact upper limit on τ from the CMB has not been worked out in detail in the literature; published constraints on the allowed abundance of A' versus lifetime only go down to $\tau = 10^{12}\,\mathrm{s}$, where the constraints are rapidly weakening, but not yet gone; see for example figure 7 of ref. [54] or figure 4 of ref. [55]. The true limit is probably somewhat lower than $10^{12}\,\mathrm{s}$; for example if $\tau_{3\gamma} < 10^{11}\,\mathrm{s}$ and $m_{A'} = 0.5\,\mathrm{MeV}$, we require $\epsilon > 4.5 \times 10^{-10}$, but since this overlaps with the BBN limits shown in figure 2 (right), this uncertainty is not important for our constraints.

Concerning limits from BBN, following the argument of section 5, the requirement for the lifetime of A' is $\tau_{e^+e^-} < 540\,\mathrm{s}$ for $m_{A'} = 1.35\,\mathrm{MeV}$ and $\tau_{3\gamma} < 3920\,\mathrm{s}$ for $m_{A'} = 0.5\,\mathrm{MeV}$. This translates into lower bounds on ϵ of 2×10^{-11} and 5×10^{-5} for scenarios **A** and **B** respectively, as displayed in figure 2 along with the other constraints derived in previous sections. These plots show that the combination of direct detection and cosmological constraints strongly disfavor $m_{A'} < 1.0\,\mathrm{MeV}$ — only when A' is heavy enough to decay at tree level are the BBN constraints on ϵ sufficiently weak for the model to be viable. Lower values of $m_{A'}$ require much larger ϵ to ensure that A' decays before disturbing BBN.

9 Conclusions

The possibility that the neutron decays into a dark fermion χ and a dark photon A' is highly constrained by an array of laboratory and astrophysical observations. The mass of χ must lie in a narrow window between 937.9 and 939.6 MeV. The mass of the A' must be greater than 1.022 MeV ($2m_e$) and less than 1.67 MeV.[4] The U(1)′ gauge coupling cannot be small (above 0.07), implying that χ comprises no more than $\sim 1\%$ of the total DM. The

[4] In an extended model, one might circumvent the lower limit on $m_{A'}$ by allowing for χ to be a long-lived unstable particle with invisible decay products, perhaps including the true dark matter of the universe. Such a framework might be able to circumvent the direct detection constraints that lead to $m_{A'} < 2m_e$ being excluded in our model.

JHEP07(2018)081

kinetic mixing parameter must lie in a rather narrow range of 10^{-11}–10^{-9}. It is intriguing that despite the many restrictions, there is still viable parameter space.

The decay mode $n \to \chi\gamma$ is still present in our model, but its rate is suppressed relative to the invisible mode by $\Gamma(n \to \chi\gamma)/\Gamma(n \to \chi A') \sim (\mu_n v')^2$ where μ_n is the neutron magnetic moment and v' is the VEV of the light scalar ϕ that breaks the U(1)$'$ symmetry. Since smaller values of v' seem less likely in view of the hierarchy problem for scalar masses, the eventual detection of the visible decay mode could be expected. Dark neutron decay could also lead to effects in nuclear processes, with ^{11}Be decays discussed as a particularly promising candidate for study in [56]. The dark matter could be discovered by direct detection, despite its small relic density. The UV completion of our model also requires heavy scalar quarks that could be accessible at LHC and detectable through their decays to first generation quarks or a jet plus missing energy.

Note added. After completion of this work, ref. [57] reported new limits on the decay channel $n \to \chi e^+ e^-$. Our model predicts such events from off-shell dark photon exchange, but at a very low rate. We computed the partial width for our benchmark models, finding $10^{-37} - 10^{-38}$ MeV, which is negligible. In addition, ref. [58] presented a new precise determination of the neutron axial vector coupling g_A using lattice QCD. This value of the coupling is lower than the experimental average determined in [10], suggesting consistency between a dark decay contribution to the neutron lifetime and g_A.

Acknowledgments

We thank S. McDermott, D. McKeen, J. Shelton, S. Reddy and D. Zhou for helpful correspondence. Our work is supported by the Natural Sciences and Engineering Research Council (NSERC) of Canada.

Open Access. This article is distributed under the terms of the Creative Commons Attribution License (CC-BY 4.0), which permits any use, distribution and reproduction in any medium, provided the original author(s) and source are credited.

References

[1] W. Mampe, L.N. Bondarenko, V.I. Morozov, Yu. N. Panin and A.I. Fomin, *Measuring neutron lifetime by storing ultracold neutrons and detecting inelastically scattered neutrons*, *JETP Lett.* **57** (1993) 82 [*Pisma Zh. Eksp. Teor. Fiz.* **57** (1993) 77] [INSPIRE].

[2] A. Serebrov et al., *Measurement of the neutron lifetime using a gravitational trap and a low-temperature Fomblin coating*, *Phys. Lett.* **B 605** (2005) 72 [nucl-ex/0408009] [INSPIRE].

[3] A. Pichlmaier, V. Varlamov, K. Schreckenbach and P. Geltenbort, *Neutron lifetime measurement with the UCN trap-in-trap MAMBO II*, *Phys. Lett.* **B 693** (2010) 221 [INSPIRE].

[4] A. Steyerl, J.M. Pendlebury, C. Kaufman, S.S. Malik and A.M. Desai, *Quasielastic scattering in the interaction of ultracold neutrons with a liquid wall and application in a reanalysis of the Mambo I neutron-lifetime experiment*, *Phys. Rev.* **C 85** (2012) 065503 [INSPIRE].

JHEP07(2018)081

[5] S. Arzumanov et al., *A measurement of the neutron lifetime using the method of storage of ultracold neutrons and detection of inelastically up-scattered neutrons*, *Phys. Lett.* **B 745** (2015) 79 [INSPIRE].

[6] J. Byrne and P.G. Dawber, *A revised value for the neutron lifetime measured using a Penning trap*, *Europhys. Lett.* **33** (1996) 187 [INSPIRE].

[7] A.T. Yue et al., *Improved determination of the neutron lifetime*, *Phys. Rev. Lett.* **111** (2013) 222501 [arXiv:1309.2623] [INSPIRE].

[8] B. Fornal and B. Grinstein, *Dark matter interpretation of the neutron decay anomaly*, *Phys. Rev. Lett.* **120** (2018) 191801 [arXiv:1801.01124] [INSPIRE].

[9] Z. Tang et al., *Search for the neutron decay $n \to X + \gamma$ where X is a dark matter particle*, arXiv:1802.01595 [INSPIRE].

[10] A. Czarnecki, W.J. Marciano and A. Sirlin, *Neutron lifetime and axial coupling connection*, *Phys. Rev. Lett.* **120** (2018) 202002 [arXiv:1802.01804] [INSPIRE].

[11] D. McKeen, A.E. Nelson, S. Reddy and D. Zhou, *Neutron stars exclude light dark baryons*, arXiv:1802.08244 [INSPIRE].

[12] G. Baym, D.H. Beck, P. Geltenbort and J. Shelton, *Coupling neutrons to dark fermions to explain the neutron lifetime anomaly is incompatible with observed neutron stars*, arXiv:1802.08282 [INSPIRE].

[13] T.F. Motta, P.A.M. Guichon and A.W. Thomas, *Implications of neutron star properties for the existence of light dark matter*, *J. Phys.* **G 45** (2018) 05LT01 [arXiv:1802.08427] [INSPIRE].

[14] K. Aitken, D. McKeen, T. Neder and A.E. Nelson, *Baryogenesis from oscillations of charmed or beautiful baryons*, *Phys. Rev.* **D 96** (2017) 075009 [arXiv:1708.01259] [INSPIRE].

[15] D. McKeen and A.E. Nelson, *CP violating baryon oscillations*, *Phys. Rev.* **D 94** (2016) 076002 [arXiv:1512.05359] [INSPIRE].

[16] R.C. Tolman, *Static solutions of Einstein's field equations for spheres of fluid*, *Phys. Rev.* **55** (1939) 364 [INSPIRE].

[17] J.R. Oppenheimer and G.M. Volkoff, *On massive neutron cores*, *Phys. Rev.* **55** (1939) 374 [INSPIRE].

[18] P. Demorest, T. Pennucci, S. Ransom, M. Roberts and J. Hessels, *Shapiro delay measurement of a two solar mass neutron star*, *Nature* **467** (2010) 1081 [arXiv:1010.5788] [INSPIRE].

[19] S. Gandolfi, J. Carlson and S. Reddy, *The maximum mass and radius of neutron stars and the nuclear symmetry energy*, *Phys. Rev.* **C 85** (2012) 032801 [arXiv:1101.1921] [INSPIRE].

[20] S. Reddy, private communication.

[21] CMS collaboration, *Search for new physics with dijet angular distributions in proton-proton collisions at $\sqrt{s} = 13$ TeV*, *JHEP* **07** (2017) 013 [arXiv:1703.09986] [INSPIRE].

[22] ATLAS collaboration, *Search for squarks and gluinos in final states with jets and missing transverse momentum using 36 fb^{-1} of $\sqrt{s} = 13$ TeV pp collision data with the ATLAS detector*, *Phys. Rev.* **D 97** (2018) 112001 [arXiv:1712.02332] [INSPIRE].

[23] Y. Aoki, T. Izubuchi, E. Shintani and A. Soni, *Improved lattice computation of proton decay matrix elements*, *Phys. Rev.* **D 96** (2017) 014506 [arXiv:1705.01338] [INSPIRE].

[24] S. Tulin and H.-B. Yu, *Dark matter self-interactions and small scale structure*, *Phys. Rept.* **730** (2018) 1 [arXiv:1705.02358] [INSPIRE].

JHEP07(2018)081

[25] G.K. Karananas and A. Kassiteridis, *Small-scale structure from neutron dark decay*, arXiv:1805.03656 [INSPIRE].

[26] S.W. Randall, M. Markevitch, D. Clowe, A.H. Gonzalez and M. Bradac, *Constraints on the self-interaction cross-section of dark matter from numerical simulations of the merging galaxy cluster* 1*E*0657-56, *Astrophys. J.* **679** (2008) 1173 [arXiv:0704.0261] [INSPIRE].

[27] D.E. Kaplan, G.Z. Krnjaic, K.R. Rehermann and C.M. Wells, *Atomic dark matter*, *JCAP* **05** (2010) 021 [arXiv:0909.0753] [INSPIRE].

[28] J. Pollack, D.N. Spergel and P.J. Steinhardt, *Supermassive black holes from ultra-strongly self-interacting dark matter*, *Astrophys. J.* **804** (2015) 131 [arXiv:1501.00017] [INSPIRE].

[29] N.F. Bell, Y. Cai and R.K. Leane, *Impact of mass generation for spin-1 mediator simplified models*, *JCAP* **01** (2017) 039 [arXiv:1610.03063] [INSPIRE].

[30] G. Steigman, B. Dasgupta and J.F. Beacom, *Precise relic WIMP abundance and its impact on searches for dark matter annihilation*, *Phys. Rev.* **D 86** (2012) 023506 [arXiv:1204.3622] [INSPIRE].

[31] M. Cirelli, P. Panci, K. Petraki, F. Sala and M. Taoso, *Dark matter's secret liaisons: phenomenology of a dark* U(1) *sector with bound states*, *JCAP* **05** (2017) 036 [arXiv:1612.07295] [INSPIRE].

[32] R.J. Scherrer and M.S. Turner, *Primordial nucleosynthesis with decaying particles. 1. Entropy producing decays. 2. Inert decays*, *Astrophys. J.* **331** (1988) 19 [INSPIRE].

[33] A. Fradette, M. Pospelov, J. Pradler and A. Ritz, *Cosmological constraints on very dark photons*, *Phys. Rev.* **D 90** (2014) 035022 [arXiv:1407.0993] [INSPIRE].

[34] J. Berger, K. Jedamzik and D.G.E. Walker, *Cosmological constraints on decoupled dark photons and dark Higgs*, *JCAP* **11** (2016) 032 [arXiv:1605.07195] [INSPIRE].

[35] M. Hufnagel, K. Schmidt-Hoberg and S. Wild, *BBN constraints on MeV-scale dark sectors. Part I. Sterile decays*, *JCAP* **02** (2018) 044 [arXiv:1712.03972] [INSPIRE].

[36] PLANCK collaboration, P.A.R. Ade et al., *Planck* 2015 *results. XIII. Cosmological parameters*, *Astron. Astrophys.* **594** (2016) A13 [arXiv:1502.01589] [INSPIRE].

[37] G. Elor, N.L. Rodd, T.R. Slatyer and W. Xue, *Model-independent indirect detection constraints on hidden sector dark matter*, *JCAP* **06** (2016) 024 [arXiv:1511.08787] [INSPIRE].

[38] CRESST collaboration, F. Petricca et al., *First results on low-mass dark matter from the CRESST-III experiment*, in 15$^{\text{th}}$ *International Conference on Topics in Astroparticle and Underground Physics (TAUP* 2017*)*, Sudbury, ON, Canada, 24–28 July 2017 [arXiv:1711.07692] [INSPIRE].

[39] R. Essig, T. Volansky and T.-T. Yu, *New constraints and prospects for sub-GeV dark matter scattering off electrons in xenon*, *Phys. Rev.* **D 96** (2017) 043017 [arXiv:1703.00910] [INSPIRE].

[40] FERMI-LAT collaboration, M. Ackermann et al., *Searching for dark matter annihilation from milky way dwarf spheroidal galaxies with six years of Fermi Large Area Telescope data*, *Phys. Rev. Lett.* **115** (2015) 231301 [arXiv:1503.02641] [INSPIRE].

[41] M. Pospelov, A. Ritz and M.B. Voloshin, *Bosonic super-WIMPs as keV-scale dark matter*, *Phys. Rev.* **D 78** (2008) 115012 [arXiv:0807.3279] [INSPIRE].

JHEP07(2018)081

[42] The GAMBIT Dark Matter Workgroup collaboration, T. Bringmann et al., *DarkBit: a GAMBIT module for computing dark matter observables and likelihoods*, *Eur. Phys. J.* **C 77** (2017) 831 [arXiv:1705.07920] [INSPIRE].

[43] E.C. Stone et al., *Voyager 1 observes low-energy galactic cosmic rays in a region depleted of heliospheric ions*, *Science* **341** (2013) 6142.

[44] AMS collaboration, L. Accardo et al., *High statistics measurement of the positron fraction in primary cosmic rays of 0.5–500 GeV with the Alpha Magnetic Spectrometer on the International Space Station*, *Phys. Rev. Lett.* **113** (2014) 121101 [INSPIRE].

[45] AMS collaboration, M. Aguilar et al., *Electron and positron fluxes in primary cosmic rays measured with the Alpha Magnetic Spectrometer on the International Space Station*, *Phys. Rev. Lett.* **113** (2014) 121102 [INSPIRE].

[46] M. Boudaud, J. Lavalle and P. Salati, *Novel cosmic-ray electron and positron constraints on MeV dark matter particles*, *Phys. Rev. Lett.* **119** (2017) 021103 [arXiv:1612.07698] [INSPIRE].

[47] J.H. Chang, R. Essig and S.D. McDermott, *Revisiting supernova 1987A constraints on dark photons*, *JHEP* **01** (2017) 107 [arXiv:1611.03864] [INSPIRE].

[48] S. Andreas, C. Niebuhr and A. Ringwald, *New limits on hidden photons from past electron beam dumps*, *Phys. Rev.* **D 86** (2012) 095019 [arXiv:1209.6083] [INSPIRE].

[49] BaBar collaboration, J.P. Lees et al., *Search for invisible decays of a dark photon produced in e^+e^- collisions at BaBar*, *Phys. Rev. Lett.* **119** (2017) 131804 [arXiv:1702.03327] [INSPIRE].

[50] S. Cassel, *Sommerfeld factor for arbitrary partial wave processes*, *J. Phys.* **G 37** (2010) 105009 [arXiv:0903.5307] [INSPIRE].

[51] J. Choquette, J.M. Cline and J.M. Cornell, *p-wave annihilating dark matter from a decaying predecessor and the galactic center excess*, *Phys. Rev.* **D 94** (2016) 015018 [arXiv:1604.01039] [INSPIRE].

[52] E. Rrapaj and S. Reddy, *Nucleon-nucleon bremsstrahlung of dark gauge bosons and revised supernova constraints*, *Phys. Rev.* **C 94** (2016) 045805 [arXiv:1511.09136] [INSPIRE].

[53] E. Hardy and R. Lasenby, *Stellar cooling bounds on new light particles: plasma mixing effects*, *JHEP* **02** (2017) 033 [arXiv:1611.05852] [INSPIRE].

[54] T.R. Slatyer, *Energy injection and absorption in the cosmic dark ages*, *Phys. Rev.* **D 87** (2013) 123513 [arXiv:1211.0283] [INSPIRE].

[55] J.M. Cline and P. Scott, *Dark matter CMB constraints and likelihoods for poor particle physicists*, *JCAP* **03** (2013) 044 [*Erratum ibid.* **05** (2013) E01] [arXiv:1301.5908] [INSPIRE].

[56] M. Pfützner and K. Riisager, *Examining the possibility to observe neutron dark decay in nuclei*, *Phys. Rev.* **C 97** (2018) 042501 [arXiv:1803.01334] [INSPIRE].

[57] UCNA collaboration, X. Sun et al., *Search for dark matter decay of the free neutron from the UCNA experiment: $n \to \chi + e^+e^-$*, *Phys. Rev.* **C 97** (2018) 052501 [arXiv:1803.10890] [INSPIRE].

[58] C.C. Chang et al., *A per-cent-level determination of the nucleon axial coupling from quantum chromodynamics*, *Nature* **558** (2018) 91 [arXiv:1805.12130] [INSPIRE].

JHEP07(2018)081